Soft Matter

RSC Publishing

PAPER

View Article Online
View Journal | View Issue

Cite this: *Soft Matter*, 2013, **9**, 7095

Calcium mediated interaction of calf-thymus DNA with monolayers of distearoylphosphatidylcholine: a neutron and X-ray reflectivity study†

Aleksandra P. Dabkowska,‡[a] Jonathan P. Talbot,‡[ab] Leide Cavalcanti,[c] John R. P. Webster,[d] Andrew Nelson,[e] David J. Barlow,[a] Giovanna Fragneto*[b] and M. Jayne Lawrence*[a]

X-ray and neutron reflection studies, the latter in conjunction with contrast variation, have been combined to study the interaction of calf thymus DNA (ctDNA) with monolayers of distearoylphosphatidylcholine (DSPC) in the presence of 20 mM Ca^{2+} ions, at the air–liquid interface as a function of surface pressure (10, 20, 30 and 40 mN m^{-1}). Analysis of the X-ray and neutron reflection data showed that, regardless of the surface pressure of the monolayer, a layer of ctDNA was present below the DSPC lipid head groups and that this ctDNA-containing layer (thickness ~12.5 to 15 Å) was separated from the DSPC head groups by a layer of water of ~9 Å thickness. The thickness of the ctDNA-containing layer was thinner than that reported for monolayers of cationic lipid at the air–water interface (18–25 Å) although in these monolayers no water layer separating the lipid head groups from the layer containing ctDNA has been reported. At all surface pressures the amount of ctDNA present in the layer was in the range 30–40% by volume. As no significant re-arrangement of the DSPC film was required to accommodate the presence of the ctDNA, this suggests that the distribution of charges in the lipid film matches well the charge spacing of ctDNA. Brewster angle microscopy measurements of DSPC on water in the absence of Ca^{2+} showed the presence of a continuous film containing small, regular shaped domains at all four surface pressures examined. When Ca^{2+} ions were present in the sub-phase, although the film was still continuous, the domains comprising the film were more irregular in appearance while the presence of Ca^{2+} ions and ctDNA resulted in the domains becoming smaller and more regularly packed on the surface.

Received 1st February 2013
Accepted 9th May 2013

DOI: 10.1039/c3sm50350j

www.rsc.org/softmatter

Introduction

The ability to artificially engineer genes means that it is now possible to tackle diseases hitherto inaccessible to traditional means of drug treatment. Although the range of clinical conditions that could benefit from gene therapy is enormous, the reality at present is that we are not yet beyond the 'proof of principle' stage. A particular stumbling block to gene therapy is that there is no effective and safe means of reproducibly ensuring delivery of the gene to its site of action within the target cell. Consequently, therefore, considerable effort has been expended in the search for suitable gene delivery vehicles or vectors. Although early gene therapy studies saw the widespread use of adenoviral and retroviral vectors, concerns over the safety of these viral-based vectors lead to more recent work focussing on the use of cationic lipids (and polymers) to form complexes known as lipoplexes (and polyplexes) with, negatively charged, plasmid DNA. In addition to their reduced toxicity, the use of lipoplexes and polyplexes to mediate gene transfer provides several advantages over viral vectors including the ability to deliver DNA to non-dividing as well as dividing cells, no limit on the size of the gene transported, and the possibility of incorporating the vector with cell specific antigens to allow for site-specific targeting.[1–3] Unfortunately, however, even though cationic lipids and polymers are less toxic than viral vectors, they do exhibit a higher degree of toxicity towards the host than is desirable, thereby limiting the amount that can be administered. An attractive alternative to the use of lipoplexes prepared from cationic lipids would be lipoplexes prepared using zwitterionic phospholipids because such vectors should not only exhibit reduced toxicities but the surface of the vectors they produce should also be readily modifiable using

[a]*Institute of Pharmaceutical Science, King's College London, The Franklin-Wilkins Building, Stamford Street, London, SE1 9NH, UK. E-mail: jayne.lawrence@kcl.ac.uk*
[b]*Institut Laue-Langevin, 6 rue Jules Horowitz, BP 156, F-38042 Grenoble Cedex, France. E-mail: fragneto@ill.fr*
[c]*European Synchrotron Radiation Facility, BP 220, 38043 Grenoble Cedex, France*
[d]*ISIS, Rutherford Appleton Laboratory, Chilton, Didcot, Oxon 0QX, UK*
[e]*ANSTO ANSTO, Locked Bag 2001, Kirrawee DC, NSW 2234, Australia*

† Electronic supplementary information (ESI) available. See DOI: 10.1039/c3sm50350j

‡ These authors contributed equally to this work.

established methodologies such as pegylation[4] to allow for longer blood circulation times and therefore slower clearance profiles of the vector.

Unfortunately, negatively charged DNA does not interact with zwitterionic phospholipids such as phosphatidylcholine and phosphatidylethanolamine,[5] although it has been shown[6] that the interaction of DNA with zwitterionic phospholipids at an interface such as that occurring at the surface of a vesicle can be mediated by the addition of condensing agents such as the divalent cations, Mg^{2+} or Ca^{2+}. As a consequence, the products of the interaction between DNA and vesicles prepared from zwitterionic lipids mediated by divalent ions have provoked interest as a means of producing non-toxic, non-viral gene delivery vehicles or vectors.[7] Perhaps surprisingly, considering the fact that the ability of phospholipids to associate with nucleic acids in presence of divalent cations is important for a number of biological processes including transcription and replication of DNA in both prokaryotic and eukaryotic cells, the nature of the complexes formed between DNA and zwitterionic phospholipids is not well understood,[8] particularly at the molecular level.[9]

Most of the work examining the interaction of DNA and zwitterionic phospholipids has focused on determining the structure of the complexes formed in solution, using for example small angle scattering, and in particular small angle X-ray scattering.[9–12] A few studies have used either X-ray[12,13,15] or more recently neutron reflectivity[16] to study the interaction of DNA with a zwitterionic lipid monolayer at the air–water interface, in the presence of a divalent cations, Mg^{2+} or Ca^{2+}. Such monolayer studies have generally used either phosphatidylethanolamine or phosphatidylcholine lipids. While phosphatidylethanolamine is often used as a helper lipid in combination with a bilayer-forming lipid when preparing lipoplexes, it is never used as sole lipid as it is unable to form the vesicles required for lipoplex preparation when used as the sole lipid. In contrast, phosphatidylcholines such as distearoylphosphatidylcholine are widely used for fabrication of vesicles suitable for preparation of range of drug and gene delivery vehicles, and these lipids are regarded as safe for human consumption. It was distearoylphosphatidylcholine, therefore, that was selected for investigation in the present study.

The work reported here involves investigations conducted using Langmuir isotherms, Brewster angle microscopy (BAM), and the combination of X-ray and neutron reflectivity (the latter in conjunction with contrast variation) to probe the interaction of calf thymus DNA (ctDNA) with monolayers of distearoylphosphatidylcholine (DSPC) in the presence of Ca^{2+}. A comparison is made between the binding of ctDNA to monolayers of the corresponding C18 cationic lipid, dimethyldioctadecyl ammonium bromide (DODAB).

Experimental

Materials

Ultrahigh quality water (resistivity 18.2 MΩ cm) from a Millipore Milli-Q system was used in all experiments. D_2O (99.9% deuteration) was either purchased from Sigma-Aldrich (Gillingham, UK) or provided by the Institut Laue-Langevin, Grenoble. The phospholipid L-α-distearoylphosphatidylcholine (DSPC) was purchased from Avanti Polar Lipids (Alabaster, USA) in three forms: fully deuterated (d_{83}-DSPC), chain deuterated (d_{70}-DSPC) and fully hydrogenous (h-DSPC). Before use, the isotopic purity of the various forms of DSPC was confirmed by determining their surface-pressure:area isotherms – no difference in the isotherm was observed for any of the isotopic forms of DSPC which all agreed with isotherms previously reported for DSPC.[17] Similarly no difference was seen in the behaviour of the isotherm if measured in D_2O as opposed to H_2O (data not shown). All lipids were used as received without further purification. Deoxyribonucleic acid from calf thymus (ctDNA) was purchased from Sigma-Aldrich (Gillingham, UK) and was spectroscopically verified to be free of protein and RNA by measuring the ratio of its UV absorbance at 260 and 280 nm. Calcium chloride (AnalaR, BDH Chemical Ltd., Poole, UK) was heated to 530 °C for 26 hours in a muffle furnace in order to remove any organic contaminants. The calcium chloride, as provided by the manufacturer, was found to lose less than 0.1% of its mass during the dry combustion process.

Langmuir isotherms

Surface-pressure area isotherms were recorded at 295 ± 2 K using a Nima 601 Langmuir trough (Coventry, UK) cleaned using chloroform, ethanol and ultrapure water. The Langmuir trough was housed in a cabinet to minimise disruption to the monolayer by air currents and to reduce airborne contamination. Three aqueous sub-phases were used in the study, namely pure water (resistivity 18.2 MΩ cm), an aqueous 20 mM $CaCl_2$ solution and solution of 20 mM $CaCl_2$ containing 0.067 mg mL^{-1} ctDNA. Prior to the addition of the DSPC to the aqueous surface, the cleanliness of the aqueous phase (volume 300 mL) was confirmed by ensuring that surface pressure, measured using a Wilhelmy plate (10 mm × 50 mm filter paper; Whatman International, Maidstone, UK) partially immersed in the subphase and attached to a pressure sensor, did not increase upon closing of the barriers. Sufficient DSPC (or an equivalent amount of deuterated DSPC) was dissolved in chloroform to produce a 2 mg mL^{-1} solution. 50 μL of this solution (Hamilton microsyringe, Sigma-Aldrich Co. Ltd., Gillingham, UK) was then added drop-wise to the surface of the appropriate aqueous subphase contained in the Langmuir trough. After addition of the DSPC to the surface of the aqueous sub-phase, a 30 min time period was left prior to compression of the monolayer (at a rate of 20 cm^2 min^{-1}) in order to ensure evaporation of the chloroform and to allow for the interaction of the ctDNA with the monolayer. The stability of the films over time was monitored at each surface pressure tested by holding the film at the required pressure and recording any change in the area of the trough over time. All films were stable for at least one hour. Isotherms were measured in triplicate to ensure reproducibility.

Brewster angle microscopy (BAM)

The BAM (BAM2plus, Nanofilm Technologie, GmbH, Goettingen, Germany) was mounted above the Langmuir trough (Nima Technology Ltd., Coventry, Warwickshire, UK), to allow for

collection of images of the morphology of the DSPC monolayer at 295 ± 2 K. The Langmuir trough (monolayer prepared as described above) and the BAM were both housed in a cabinet to minimise disruption to the monolayer by air currents and to reduce airborne contamination. BAM experiments were performed on monolayers compressed (at a speed of 20 cm^2 min^{-1}) to surface pressures of 10, 20, 30, 40 and, where possible, 50 mN m^{-1}. The monolayers films were stable at each of the surface pressures examined for the period of the BAM experiment. P-polarised light (supplied by an NDYAG laser operating at a wavelength of 532 nm) was emitted by the BAM onto the water surface at an angle of incidence of the Brewster angle for water (53.15°) and the light reflected from the surface collected by two achromatic lenses and detected with a CCD camera. The CCD camera converted the reflectivity signal from the sample into a video image. Calibrations were performed by obtaining images of the bare water surface prior to spreading of the monolayer. These 'background images' were subtracted from the sample images taken subsequently in order to obtain sharper pictures of the monolayer films. The spatial resolution of the BAM is approximately 2 μm. At the low magnification of ×10 employed during this study, the images represent a sample size of 430 μm (vertical field of view) × 530 μm (horizontal field of view). The BAM images reported here were obtained from freshly prepared and compressed monolayers. Images were obtained from three freshly prepared monolayer films to ensure reproducibility.

Neutron reflectivity

Neutron reflectivity (NR) measurements at the air–liquid interface were performed on the ISIS reflectometer, SURF, at the Rutherford Appleton Laboratory, UK. The time-of-flight (TOF) method was used with neutron wavelengths in the range 0.05 to 6.5 Å with the beam inclined at 1.5° to the horizontal to provide a momentum transfer, Q, (where $Q = 4\pi\sin\theta/\lambda$, where θ and λ are respectively the angle of incidence, relative to the plane of the surface and the wavelength of the incident neutrons) in the range of 0.05 to 0.5 $Å^{-1}$. Beam intensities were calibrated with respect to D_2O. A flat background (determined by extrapolation to high momentum transfer) was subtracted from all reflectivity profiles.

Monolayers of the various isotopic forms of DSPC were prepared as detailed using a Nima 601 Langmuir trough (Nima Technology Ltd., Coventry, UK) mounted on the SURF beamline and housed under a Perspex cover to minimise monolayer disruption by air currents and to reduce airborne contamination. NR measurements were made at 295 ± 2 K. A range of aqueous sub-phases were used, these were either D_2O or air-contrast-matched-water (acmw), with and without 20 mM $CaCl_2$ and in the case of sub-phases containing 20 mM $CaCl_2$ with and without 0.067 mg mL^{-1} ctDNA. Acmw has a neutron scattering length density equivalent with that of air and contains 8.1 vol% D_2O in H_2O. When calcium chloride was present in the sub-phase the subscript $CaCl_2$ denotes its presence. It should be noted that the amount of calcium chloride used in the present study was insufficient to change the (neutron) SLD of the relevant aqueous phase. NR measurements were performed at 4 surface pressures, namely 10, 20, 30 and 40 mN m^{-1} for 3 contrasts of lipid and aqueous sub-phase, namely d_{70}-DSPC on acmw, d_{83}-DSPC on acmw and d_{70}-DSPC on D_2O – in the absence and presence of $CaCl_2$ and, where required, ctDNA. The monolayers films were stable (in terms of surface area) at each of the surface pressures examined for the totality of the neutron reflectivity experiment.

X-ray reflectivity

X-ray reflectivity (XR) measurements were made on the ID10B beamline at the ESRF, Grenoble, France. The custom built in-house Langmuir trough was used in the same manner as described for the neutron reflectivity experiments. A monochromatic X-ray wavelength, $\lambda = 0.13838$ nm was selected by a Ge(111) crystal. Reflectivity measurements were performed over a range of angles to give a momentum transfer ranging from the critical angle of total reflection of the air–water interface to 0.62 $Å^{-1}$. The reflected beam was detected by a linear position-sensitive detector (PSD-50 M, Braun, Garching, Germany) that records an intensity profile as a function of the vertical scattering angle. The spectrum obtained at each given angle of incidence was fitted by a function comprising a Gaussian and a linear slope, with the reflected intensity given by the integral of the Gaussian. The diffuse scattering component was then subtracted.

The custom built in-house Langmuir trough was used in the same manner as described for the neutron reflectivity experiments. The Langmuir trough was sealed in a water-saturated helium filled chamber to reduce sub-phase evaporation and parasitic background scattering from air. X-ray reflectivity experiments were performed at 295 ± 2 K on h-DSPC monolayers spread either on H_2O or D_2O containing 20 mM $CaCl_2$ with and without 0.067 mg mL^{-1} ctDNA and compressed (at a speed of 20 cm^2 min^{-1}) to the final maintained surface pressures of 5, 20, 30 and 40 mN m^{-1}. The monolayers films were stable at each of the surface pressures examined for the period of the X-ray reflectivity experiment, typically 30 minutes. The presence of 20 mM calcium chloride in the sub-phase was denoted by the subscript $CaCl_2$. It should be noted that the amount of calcium chloride used in the present study was insufficient to significantly change the X-ray scattering length, Nb, of the aqueous sub-phase.

As part of the present study the effects of H/D substitution on molecular geometry and hydration were performed using X-ray reflectivity which is unaffected by changes in atomic nuclei as scattering only arises from the electrons orbiting the nuclei. X-ray reflectivity curves for h-DSPC on sub-phases of H_2O and D_2O were found to be comparable as were the X-reflectivity curves showing the Ca^{2+}-mediated interaction of h- and d-chromosomal DNA, supporting the hypothesis that the deuteration of various components of the system did not significantly alter the structure of the monolayer (data not shown).

Data analysis

Analysis of the reflectivity profiles was performed using the Abeles matrix method to calculate the measured reflectivity profiles by creating a model to approximate the interfacial structure normal to the surface by means of stacked layers (or

Table 1 Scattering lengths and scattering length densities used for fitting the neutron and X-ray data

Material	Molecular formula	Molecular volume (Å^3)	Scattering length[a] (10^{-4} Å)	NR scattering length density[b] (10^{-6} Å^{-2})	XR scattering length density[b] (10^{-6} Å^{-2})
h-DSPC chains	$C_{34}H_{70}$	980[c]	−3.59	−0.37	7.85
d-DSPC chains	$C_{34}D_{70}$	980[c]	69.29	7.07	N/D
h-DSPC head group	$C_{10}H_{18}NO_8P$	344[d]	6.00	1.75	13.4
d-DSPC head group	$C_{10}H_5D_{13}NO_8P$	344[d]	19.54	5.68	N/D
Water	D_2O	30[e]	1.905	6.35	9.37
	H_2O	30[e]	−0.168	−0.56	9.37
DNA				3.67 (H_2O)[f]	14.9
				4.46 (D_2O)[f]	

[a] Calculated from the atomic scattering lengths of the constituent atoms. [b] Calculated as the scattering length of the moiety divided by its molecular volume. [c] Calculated as described by Armen.[19] [d] The volume of the PC head group was calculated as the sum of the volumes of phosphate, glycerol, carbonyl and choline.[19] [e] The volume of H_2O/D_2O was assumed to be 30 Å^3 from reported simulation data[20] where water was calculated to have a volume of 30.4 Å^3. [f] The SLD of the calf thymus DNA (DNA) was calculated assuming a composition of 41.9% G–C and 58.1% A–T content (as determined by the manufacturer). Note that when modelling the SNR data, the SLD of the ctDNA was calculated taking into account the differential exchange of its labile protons (Jacrot 1972) and was therefore dependent on whether the sub-phase was air-contrast matched water or D_2O. Exchange of labile H's in nucleotides in D_2O were as reported by Jacrot.[21] N/D = not determined.

slabs) of thickness, d_n, scattering length density (SLD), ρ_n, and roughness, $\sigma_{n,n+1}$ sandwiched between the super- and sub-phases. It is preferable to use the least number of layers possible to fit the reflectivity curves, with constraints applied to limit the fitted parameters to physically reasonable values. The SLD of a layer (or slab) is defined by 3 parameters; the sum of the scattering lengths of the atoms comprising the lipid (component) or DNA in the layer, the volume occupied by the lipid (component) or DNA, and the volume of solvent penetrating the layer. Splitting the SLD of each layer in this way enables the volume of each component together with the solvent fraction to be linked across the various contrasts studied while data fitting. Thicknesses' of the DSPC hydrocarbon chain region and head group were constrained to be in the range 10–50 Å and 8–12 Å, respectively. Unless stated otherwise, the roughness between the various layers in the model was fixed at physically plausible values of 3.5–4.5 Å. Table 1 lists the SLDs used in the fitting routines for the various contrast systems studied. Refinement of both the multiple neutron contrast data and the X-ray data was performed using MOTOFIT using genetic optimization.[18]

Results and discussion

Langmuir isotherms

In order to investigate the Ca^{2+} mediated interaction of the zwitterionic phospholipid, h-DSPC, with ctDNA a Langmuir isotherm was used to establish the variation in the (apparent) interfacial area per DSPC molecule, A_0, as a function of surface pressure, π at the experimental temperature of 295 ± 2 K. Shown in Fig. 1 are the Langmuir (π–A_0) isotherms obtained for h-DSPC on H_2O, h-DSPC on a sub-phase of 20 mM $CaCl_2$ in H_2O and h-DSPC on a sub-phase of H_2O containing 20 mM $CaCl_2$ and 0.067 mg mL^{-1} ctDNA.

DSPC π–A_0 isotherm

In agreement with others,[17] the π–A_0 isotherm obtained for a monolayer of h-DSPC on H_2O at 295 ± 2 K in the present study is consistent with that of a gel phase, L_β, lipid over the whole of the range of surface pressures up to the monolayer collapse point, which occurred at a surface pressure of ~60 mN m^{-1}. For example, the lift off area for the DSPC monolayer occurred at the relatively small area per molecule of ~52 Å^2, and the area per DSPC molecule only slightly decreased to ~45 Å^2 upon compression to a surface pressure of 40 mN m^{-1}. If the isotherm is extrapolated to its collapse point, a limiting interfacial area per molecule of ~42 Å^2 is obtained, which is precisely what would be expected given that the limiting cross-sectional area for each of the molecules' two octadecyl chains would be 21 Å^2, further supporting the hypothesis that DSPC is in the gel phase under the conditions of the experiment.

The π–A_0 isotherms of the other 'contrasts' used in the neutron reflectivity study, namely d_{70}-DSPC on water and acmw, d_{83}-DSPC on acmw and h-DSPC on D_2O, were also determined (data not shown) both to check the purity of the various isotopic forms of the lipid and to verify that deuteration of either the DSPC molecule or the aqueous sub-phase did not cause any significant alteration in surface behaviour – a result which is important for the subsequent X-ray and neutron reflection studies. As expected, because the DSPC did not undergo a phase transition under the conditions of the experiment, the isotherm of the deuterated and protiated versions of lipid, when spread on either H_2O or D_2O, were superimposable within experimental error.[22,23]

Effect of calcium ions and DSPC on the DSPC π–A_0 isotherm

As can be seen in Fig. 1, at low surface pressures of ~10 to 20 mN m^{-1}, the π–A_0 isotherm of h-DSPC prepared in the presence of 20 mM $CaCl_2$ was slightly more expanded than the one prepared in its absence. For example lift off occurred at an area per DSPC molecule of ~55 Å^2 in the presence of Ca^{2+} and at ~52 Å^2 in its absence. At higher surface pressures however, the π–A_0 isotherm was more similar to that obtained in the absence of Ca^{2+}. Although the monolayer of DSPC formed in the presence of Ca^{2+} was more stable than that formed in its absence, collapsing at a surface pressure of ~65 mN m^{-1} as opposed to ~60 mN m^{-1}. Despite the slightly expanded nature of the

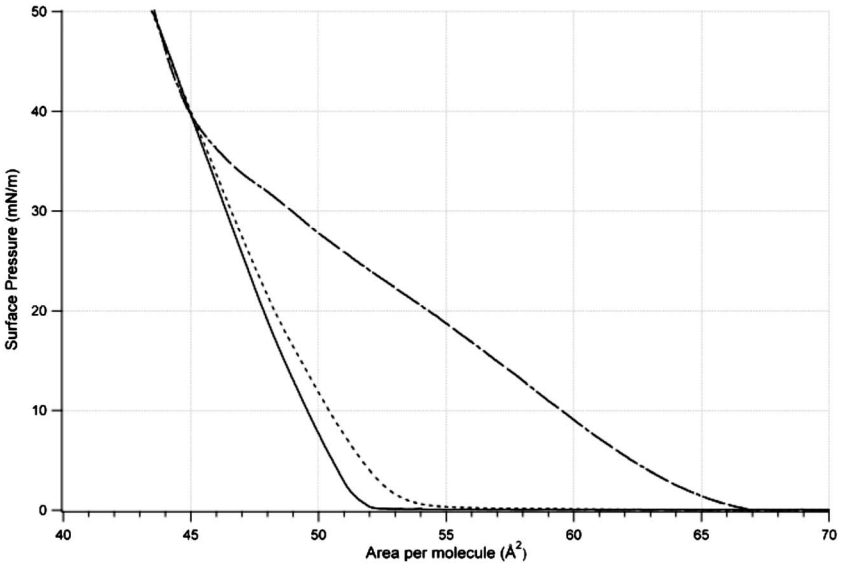

Fig. 1 (a) Surface pressure-area isotherms of h-DSPC on a aqueous sub-phase [solid line], an aqueous sub-phase containing 20 mM $CaCl_2$ sub-phase without [dotted line] and with [dot-dash line] calf-thymus DNA (0.067 mg mL^{-1}) at 298 ± 2 K. Number of repeats (n) = 3.

h-DSPC monolayer spread on the aqueous phase containing 20 mM $CaCl_2$ at low surface pressures, the lipid is still considered to be in the gel phase.

In contrast, when a h-DSPC monolayer was spread on a sub-phase containing both 20 mM $CaCl_2$ and 0.067 mg mL^{-1} ctDNA, a much more expanded isotherm was observed at all surface pressures up to ~40 mN m^{-1}. Note that as the area per molecule calculated in the presence of ctDNA and $CaCl_2$ assumes that only lipid was present at the surface, this result may suggest a re-arrangement of the DSPC monolayer. Significantly, no difference in the π–A_0 isotherm of the h-DSPC monolayer on water containing ctDNA but no calcium was seen compared to that obtained with h-DSPC monolayer on water (data not shown), supporting the hypothesis that calcium mediates the interaction of ctDNA with the DSPC monolayer. In this context it is worth commenting that there was no evidence that the ctDNA itself exhibited any surface activity, at least at the concentrations used in the present study as surface tension measurements showed that ctDNA did not cause any reduction in the surface tension of the appropriate sub-phase.

At surface pressures above 30 mN m^{-1}, the effect of calcium mediated ctDNA interaction with the DSPC monolayer was diminished, suggesting that at higher pressures, the interaction of ctDNA with the DSPC monolayer is reduced. Ultimately, at a surface pressure of just over 50 mN m^{-1}, the DSPC monolayer formed in the presence of ctDNA and Ca^{2+} collapses at a lower pressure than that seen with a monolayer of DSPC on water or water-containing $CaCl_2$ suggesting, possibly surprisingly, that the mixed DSPC/Ca^{2+}/ctDNA film is less stable.

Brewster angle microscopy (BAM)

At extremely low surface pressures of <0.5 mN m^{-1} islands of (light) condensed h-DSPC phase were visible on the (dark) water surface (data not shown). At surface pressures of ~1 mN m^{-1} the individual patches of condensed h-DSPC came together to give the appearance of a continuous film of small, relatively uniformly shaped, domains of approximately 10 μm which, while "apparently" packing slightly more tightly together, retained their identity upon compression as would be expected for a monolayer that was in the L_β phase and did not undergo a phase transition during compression.

The BAM images of a h-DSPC monolayer spread on a sub-phase of water at the surface pressures of 10, 20, 30, 40 and 50 mN m^{-1} are shown in Fig. 2a, d, g, j and m, respectively. Similar BAM images have been reported for DSPC monolayers on an aqueous sub-phase.[24–27] Sanchez and Badia[27] have attributed the appearance in the BAM images of small, relatively uniformly shaped, domains to variations in reflected light intensity (grey levels) arising from optical anisotropy induced by different tilt-azimuthal orientations of the DSPC molecules. Other possible reasons for the variation in reflectivity, including the formation of a monolayer of inhomogeneous thickness or variations in the long-range molecular orientation, were considered unlikely as neither the molecular area nor the alkyl chain tilt of DSPC varies much with surface pressure.[27] However, even if the differences in reflected light intensity were due to differences in monolayer thickness or alkyl chain tilt, the size of the domains were sufficiently small, *i.e.* less than 10 μm in diameter, that from the point of view of the reflectivity measurements reported below, that they should not pose a problem as the size of each domain was smaller than the coherent length of the beams used. Consequently any diffuse scattering arising from these domains would not be expected to contribute significantly to the measured reflectivity. Therefore the results of the analysis of the reflectivity data can be reasonably assumed to represent an average over the DSPC monolayer.

The addition of 20 mM calcium chloride to the aqueous sub-phase caused the domains observed using BAM to become more irregular in appearance as seen in Fig. 2b, e, h, k and n

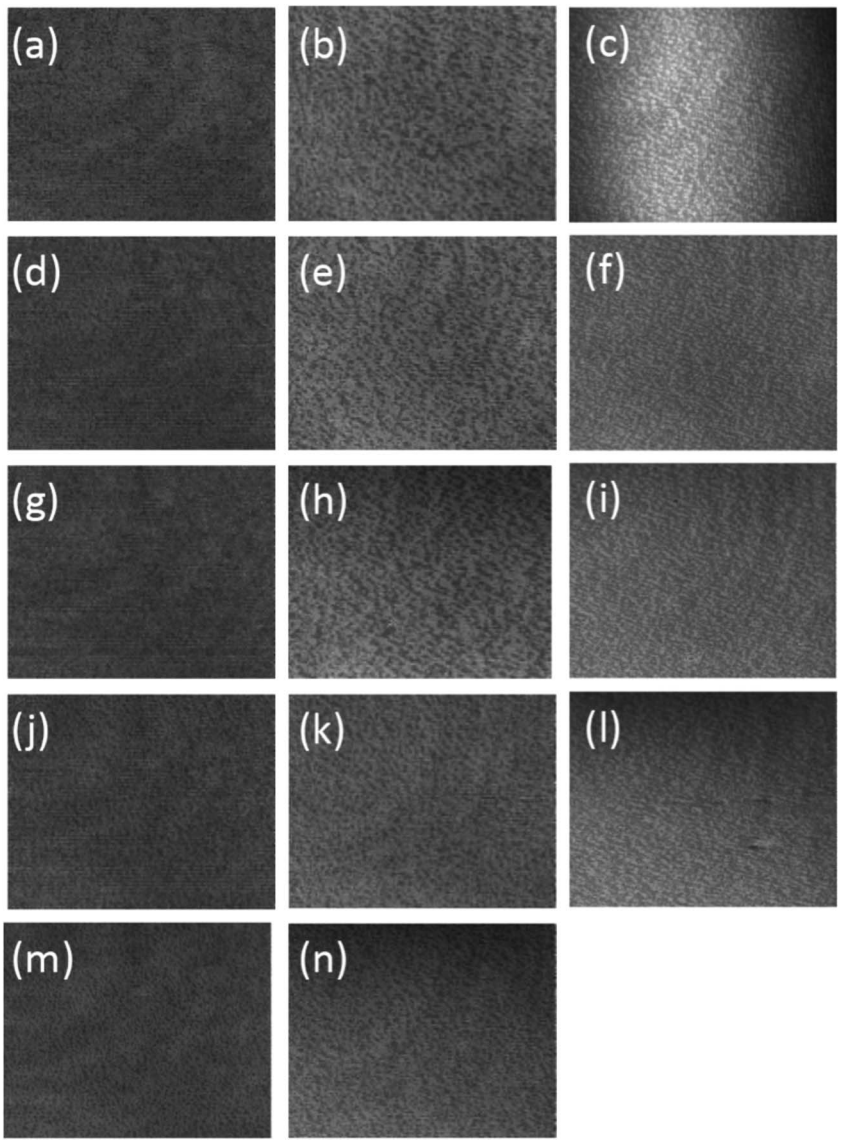

Fig. 2 BAM images of DSPC monolayer spread on pure water (a, d, g, j and m), an aqueous solution of 20 mM $CaCl_2$ (b, e, h, k and n) and an aqueous solution of 20 mM $CaCl_2$ containing 0.067 mg mL^{-1} DNA (c, f, i and l) at 295 ± 2 K and compressed to 10, 20, 30, 40 and 50 mN m^{-1}, respectively. The size represented by each image is 430 μm (vertical) ×538 μm (horizontal). Experiment resolution is ~2 μm.

(corresponding to surface pressures of 10, 20, 30, 40 and 50 mN m^{-1}, respectively). This change in the appearance of the domains was most noticeable at very low surface pressures, where the greatest difference in surface pressure was noticed between the films formed in the absence and presence of Ca^{2+}. Upon compression the integrity of the domains remained largely unchanged upon compression as would be expected for a monolayer that was in the L_β phase and did not undergo a phase transition during compression. The presence of both Ca^{2+} and ctDNA in the aqueous sub-phase caused a further change in the appearance of the domains comprising to film which become smaller and more regular (Fig. 2c, f, i and l, corresponding to surface pressures of 10, 20, 30 and 40 mN m^{-1}, respectively, 50 mN m^{-1}), although the domains were still not as small and as regular as seen for h-DSPC on pure water. Note that because the DSPC monolayer formed in the presence of ctDNA and Ca^{2+} collapses at a surface pressure just above 50 mN m^{-1} it was not possible to compress.

Reflectivity measurements

Effect of calcium on monolayer structure. The effect on the structure of the DSPC monolayer of the calcium-mediated interaction of ctDNA was studied in detail using a combination of X-ray and neutron reflection in combination with contrast variation.

Firstly, however, the effect of Ca^{2+} on the structure of the DSPC monolayer was determined as a function of surface pressure using the three neutron reflectivity contrasts, d_{70}-DSPC on acmw ($\pm Ca^{2+}$), d_{83}-DSPC on acmw ($\pm Ca^{2+}$) and d_{70}-DSPC on D_2O ($\pm Ca^{2+}$). Since there were no X-ray data collected for the DSPC monolayers spread on the sub-phases of pure H_2O or D_2O,

X-ray reflectivity data were not included in the analyses of these systems.

The analyses of the three neutron reflection data sets for the DSPC monolayers were found to be well fitted using a two-layer model of different SLD corresponding to the alkyl chains region and the lipid head groups. Tables 2 and 3 give the parameters obtained from this analysis with Table 2 giving the fit parameters for the DSPC monolayer in the absence of calcium ions and Table 3 showing the corresponding parameters for the DSPC monolayer in the presence of calcium ions. Note that the neutron reflectivity data for a DSPC monolayer on water at a surface pressure of 10 mN m^{-1} were not collected in this study. The reflectivity curves with the SLD profiles for the DSPC monolayer in the absence of calcium ions are shown in Fig. 3, while the corresponding fits for the DSPC monolayer in the presence of calcium ions are shown in ESI, Fig. 1.†

As can clearly be seen from a comparison of the data given in Tables 2 and 3, the presence of Ca^{2+} in the sub-phase causes no significant changes in the structure of the DSPC monolayer, regardless of the surface pressure of the film – despite there being a very slight increase in the surface pressure of the DSPC film in the presence of Ca^{2+}, particularly at low values of surface pressure. Furthermore, as would be expected for a lipid in its condensed, L_β phase, the thickness of the DSPC hydrocarbon layer of DSPC increased only very slightly upon compression (from ~19 Å at 20 mN m^{-1} up to ~20 to 21 Å at 40 mN m^{-1}). In addition, neither the thickness nor the hydration of the head group region changed significantly as a function of pressure or in the presence of Ca^{2+}.

Using the fitted values of the DSPC alkyl chain layer thicknesses (and assuming an alkyl chains' volume of 980 $Å^3$), the calculated molecular interfacial areas, A_0, are obtained as 45 ± 2 $Å^2$ and 43 ± 2 $Å^2$, at 20 mN m^{-1} and 40 mN m^{-1}, respectively, for the DSPC monolayers spread on pure water; the corresponding areas for the monolayers spread above a sub-phase containing 20 mM Ca^{2+} are closely similar – obtained as 43 ± 2 $Å^2$ and 41 ± 2 $Å^2$, respectively. These values of interfacial area are consistent with those derived from the corresponding π–A_0 isotherms.

Given that the fitted alkyl chain layer thicknesses are somewhat smaller than the fully extended length of a C17 chain (~22 Å, calculated from 1.5 + 1.265n where n is the number of chain carbons[28]), these data (Tables 2 and 3) also suggest that despite the fact that the DSPC exists here in the gel phase, the lipid molecules are nevertheless tilted with respect to the normal to the interface (by ~20°), even in the case of the monolayers maintained at 40 mN m^{-1}. Furthermore, given that the fully extended length of a glycerophosphatidylcholine group is cited[29] as 10.5 Å, our estimate of ~11 indicates that the DSPC head groups must lie parallel to the interface normal, each projecting vertically down into the aqueous subphase.

Simultaneous fits to the combined X-ray and neutron reflectivity data for the DSPC monolayers spread on sub-phases containing 20 mM Ca^{2+} (ESI, Fig. 2†) gave fitted parameter values (shown in Table 4) that were broadly consistent with those obtained from fitting the neutron data alone, although the quality of the fit obtained for d_{70}-DSPC on D_2O was noticeable poorer. The inclusion of the X-ray data leads to a rather more wet head group layer (with 43–54% *vs.* 36–41% water content). Note that the quality of the fit obtained for the X-ray reflectivity was poor in the Q range 0.1–0.2 $Å^{-1}$ and while the quality of the fit could be greatly improved by using a lower alkyl chain volume of 870 $Å^3$, the parameters used to obtain this fit were not significantly different from those obtained using the higher value of 980 Å.

Effect of calcium and DNA on monolayer structure. The addition of ctDNA to the DSPC monolayers spread on a Ca^{2+}-containing sub-phase was found to cause significant changes in both the X-ray and neutron reflectivity curves (see Fig. 4, 5). By way of contrast it should be noted that neutron and X-ray experiments performed in the presence of ctDNA but in the absence of $CaCl_2$ showed no change in reflectivity resulting from the addition of ctDNA, clearly indicating that the presence

Table 2 Structural parameters derived from optical matrix fitting of a two-layer model to neutron reflectivity data for a DSPC monolayer (d_{70}-DSPC on acmw, d_{83}-DSPC on acmw and d_{70}-DSPC on D_2O) on a pure water sub-phase at[a] 295 ± 2 K

Surface pressure (mN m^{-1})	20	30	40
Chain thickness (Å)	18.9 ± 0.2	18.8 ± 0.3	20.1 ± 0.2
Solvent (%)	0	0	0
Head thickness (Å)	10.3 ± 0.5	11.2 ± 0.3	10.7 ± 0.5
Solvent (%)	34 ± 3	39 ± 4	35 ± 3
Water/lipid	6	7	6
Area per DSPC molecule ($Å^2$)	45 ± 2	42 ± 2	43 ± 2

[a] Solvent (%) is the % of the volume of the layer occupied by solvent, here water. The number of water molecules per head group was estimated from the fitted volume of hydration, using the molecular volumes of the head group and water. Area per DSPC molecule was calculated from the molecular volume of the entire molecule with the associated water divided by the thickness of sum of the head and chains region as determined by neutron reflectivity measurements.

Table 3 Structural parameters derived from optical matrix fitting of a two-layer model to neutron reflectivity data for a DSPC monolayer (d_{70}-DSPC on acmw, d_{83}-DSPC on acmw and d_{70}-DSPC on D_2O) on sub-phase containing 20 mM $CaCl_2$ at[a] 295 ± 2 K

Surface pressure (mN m^{-1})	10	20	30	40
Chain thickness (Å)	17.4 ± 0.2	18.8 ± 0.3	20.1 ± 0.2	20.7 ± 0.2
Solvent (%)	0	0	0	0
Head thickness (Å)	12.0 ± 0.7	11.0 ± 0.8	11.4 ± 0.8	11.4 ± 0.9
Solvent (%)	43 ± 5	38 ± 6	35 ± 7	36 ± 7
Water/lipid	9	7	6	6
Area per DSPC molecule ($Å^2$)	46 ± 2	43 ± 2	42 ± 2	41 ± 2

[a] Legends as per Table 2.

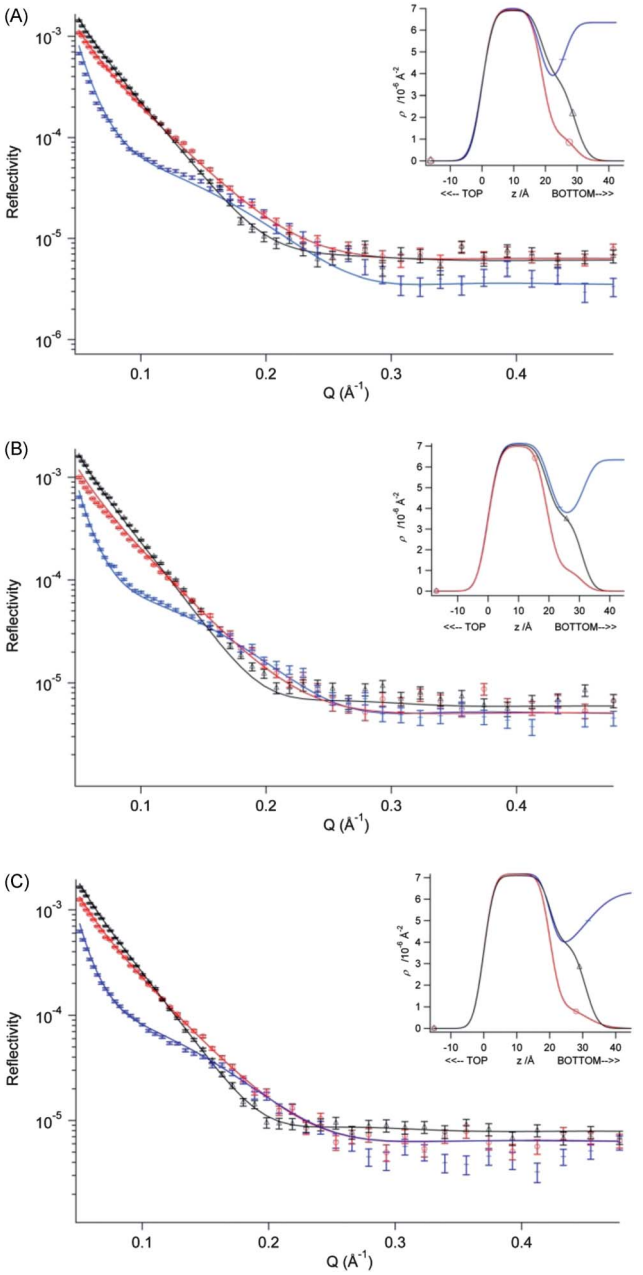

Fig. 3 Fitted profiles for DSPC monolayers on a pure water sub-phase at 298 ± 2 K obtained from fitting a two-layer model to three NR contrasts of a DSPC monolayer, d_{70}-DSPC on acmw (red), d_{83}-DSPC on acmw (black) and d_{70}-DSPC on D_2O (blue). The surface pressures shown are (A) 20 mN m^{-1}, (B) 30 mN m^{-1} and (C) 40 mN m^{-1}. Inset to each figure shows the scattering length density profiles calculated from the fit to that data set as a function of the interface in the *z*-direction.

of calcium is a pre-requisite for DNA binding to the phospholipid monolayer.

Whereas there are no Bragg peaks seen in the reflectivity profiles recorded for the DSPC monolayers exposed to ctDNA in the presence of Ca^{2+} – from which it is inferred that the addition of ctDNA does not lead to any formation of multilayers – it nevertheless proved impossible to fit the data obtained in the presence of ctDNA using the same two layer model as was used for the systems with ctDNA absent. Satisfactory fits (Fig. 4) could

Table 4 Structural parameters derived from optical matrix fitting of a two-layer model to three contrasts of neutron reflectivity data (d_{70}-DSPC on acmw, d_{83}-DSPC on acmw and d_{70}-DSPC on D_2O) and one contrast of X-ray reflectivity data (h-DSPC on H_2O) for a DSPC monolayer spread on a sub-phase containing 20 mM $CaCl_2$ at[a] 295 ± 2 K

Surface pressure (mN m^{-1})	10	20	30	40
Chain thickness (Å)	18.6 ± 1	18.8 ± 1	19.5 ± 1	19.2 ± 1
Solvent (%)	0	0	0	0
Head thickness (Å)	9.8 ± 1	9.5 ± 1	9.2 ± 1	10.3 ± 1
Solvent (%)	54 ± 5	44 ± 4	35 ± 5	43 ± 4
Water/lipid	13	9	6	9
Area per DSPC molecule (Å^2)	46 ± 2	47 ± 2	46 ± 2	45 ± 2

[a] Legends as per Table 2.

only be obtained by assuming the presence of (at least) three sub-layers within the monolayer. Table 5 shows the structural parameters for a three-layer model obtained through simultaneous fitting of the neutron and X-ray reflectivity for a DSPC monolayer on a sub-phase containing 20 mM $CaCl_2$ and ctDNA. In the model used, the first layer is assumed to contain the lipid alkyl chains, the second, the hydrated lipid head groups, and the last layer, hydrated ctDNA. The corresponding parameters obtained through fitting just the three contrasts of neutron reflectivity data yielded roughly similar results (see ESI, Table 1†) but with a slightly thicker head group layer (as was seen in the modelling of the reflectivity data for the DSPC monolayer without ctDNA, ~12 Å *vs.* ~9 Å), and a slightly greater level of solvent in the ctDNA layer (85–90% *vs.* ~75%). Assuming the presence of calcium ions in the head region (at the level of one calcium ion/phospholipid head group) did not improve the fit obtained for the reflectivity data. Indeed the difference in the X-ray scattering length density is small – 9.37 for pure water and 9.57 for water containing 2 M $CaCl_2$ (*i.e.* a 100 fold increase in concentration over that in the bulk solution). Furthermore, it is of note that roughness on the DNA, that is, the roughness between the DNA and the adjacent head groups tends during fitting to unreasonably high values. In addition it was still possible to fit the roughness at the other interfaces using a value in the range 3.5–4.5 Å.

With the model as summarised in Table 5, the fit to the X-ray reflectivity data, whilst reasonable, was not ideal, and further modelling was performed assuming a four-layer model – with an intervening solvent layer inserted between the lipid head groups and the ctDNA layers. The fits to the neutron reflectivity profiles were barely altered by this change, but there were significant improvements seen for the fits to the X-ray reflectivity profiles (see Fig. 5). The values of the fitted parameters for this four-layer model are presented in Table 6. It is of note that while the quality of fit of the X-ray reflectivity data improved upon addition of the additional water layer, it made little difference to the fit parameters for the lipid layer.

The solvent layer intervening the head groups and ctDNA layers was fitted with a thickness of ~9 Å, and the addition of this sub-layer to the model served to reduce the thickness of the hydrated ctDNA layer from 23–28 Å to ~16 Å. This reduced DNA layer thickness is consistent with the results published by

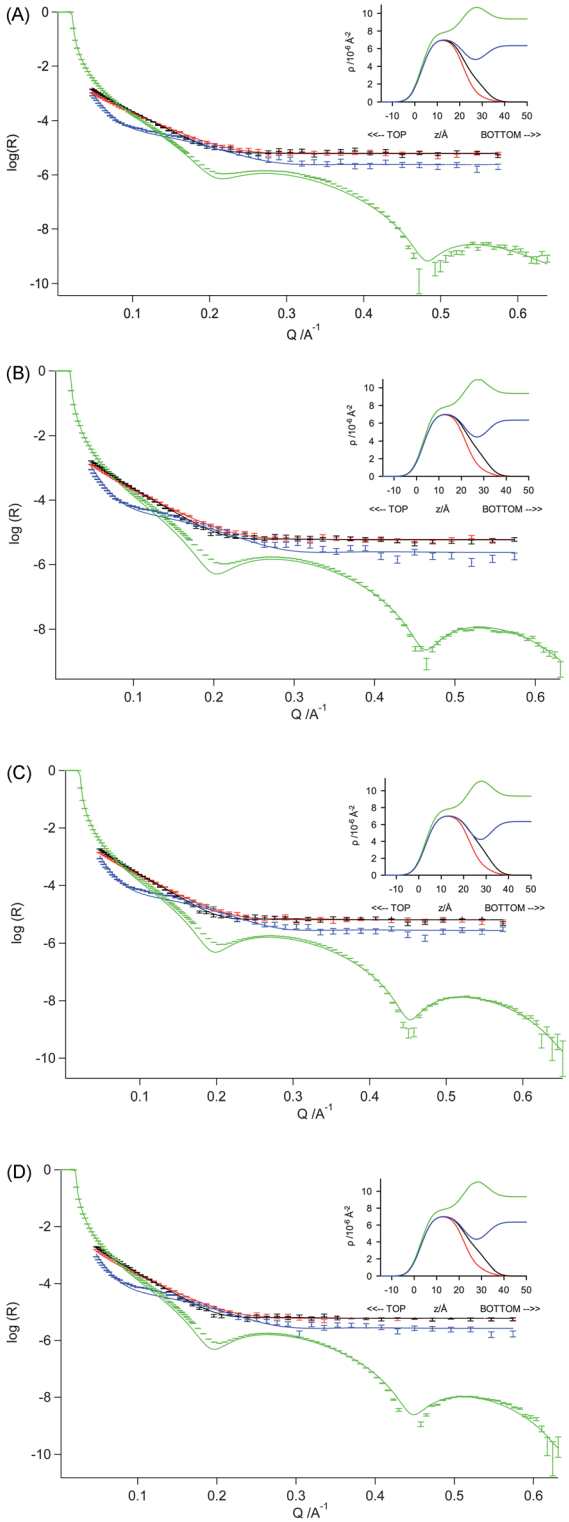

Fig. 4 Measured and fitted reflectivity profiles for DSPC monolayers on a subphase containing 20 mM $CaCl_2$ at 295 ± 2 K – with simultaneous optical matrix fitting of a three-layer model using the neutron reflectivity data for d_{70}-DSPC on acmw (red), d_{83}-DSPC on acmw (black) and d_{70}-DSPC on D_2O (blue), and X-ray reflectivity data for h-DSPC on H_2O (green). The monolayers were maintained at surface pressures of (A) 10 mN m^{-1}, (B) 20 mN m^{-1}, (C) 30 mN m^{-1} and (D) 40 mN m^{-1}.

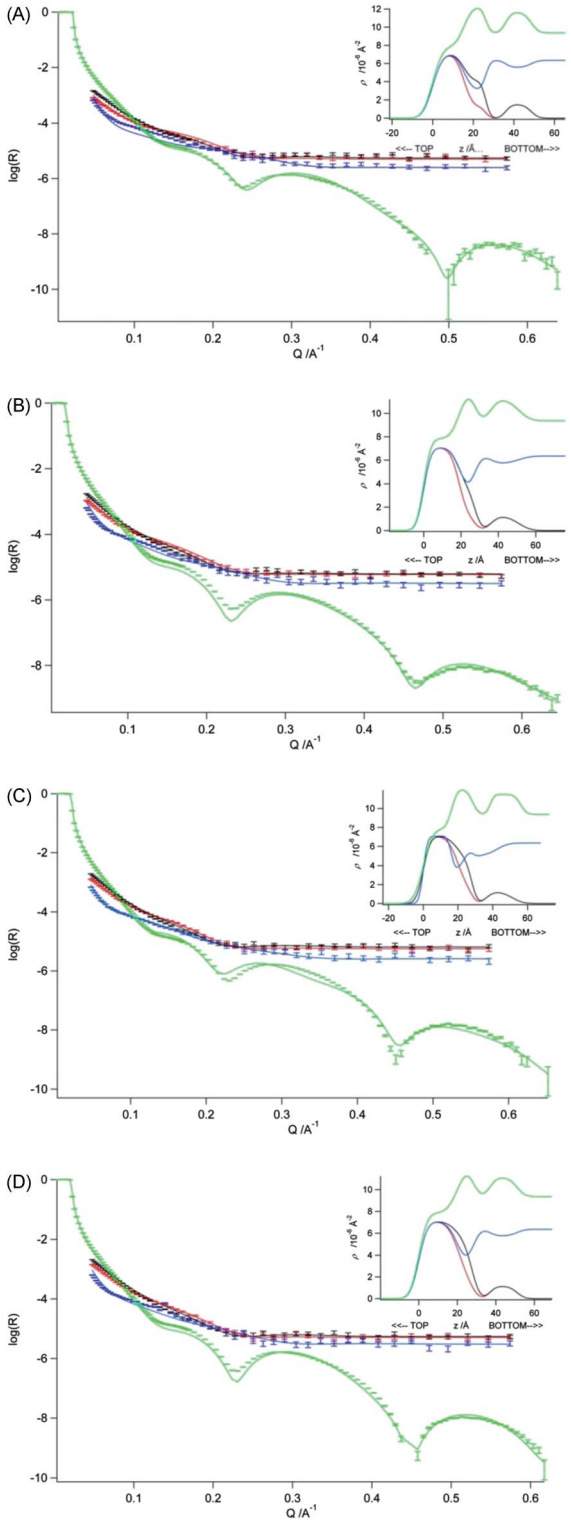

Fig. 5 Measured and fitted reflectivity profiles for DSPC monolayers on a subphase containing 20 mM $CaCl_2$ and ctDNA (0.067 mg mL^{-1}) at 295 ± 2 K – with simultaneous optical matrix fitting of a four-layer model using the neutron reflectivity data for d_{70}-DSPC on acmw, d_{83}-DSPC on acmw and d_{70}-DSPC on D_2O, and the X-ray reflectivity data for h-DSPC on H_2O. The monolayers were maintained at the surface pressures of (A) 10 mN m^{-1}, (B) 20 mN m^{-1}, (C) 30 mN m^{-1} and (D) 40 mN m^{-1}. Inset to each figure shows the scattering length density profiles calculated from the fit to that data set as a function of the interface in the *z*-direction.

Table 5 Structural parameters derived through fitting a three-layer optical matrix model to three contrasts of neutron reflectivity data (d_{70}-DSPC on acmw, d_{83}-DSPC on acmw and d_{70}-DSPC on D_2O) and one contrast of X-ray reflectivity data (h-DSPC on H_2O) for DSPC monolayers spread on a sub-phase containing 20 mM $CaCl_2$ and ctDNA (0.067 mg mL^{-1}) at 295 ± 2 K[a]

Surface pressure (mN m^{-1})	10	20	30	40
Chain thickness (Å)	17.7 ± 0.4	18.2 ± 0.3	19.6 ± 0.4	19.4 ± 0.5
Solvent (%)	0	0	0	0
Head thickness (Å)	8.9 ± 0.8	9.3 ± 0.44	8.6 ± 0.5	9.2 ± 0.6
Solvent (%)	51 ± 7.0	42 ± 5	29 ± 7	34 ± 7
Water/lipid	12	8	5	6
Area per DSPC molecule ($Å^2$)	50 ± 2	48 ± 2	47 ± 2	46 ± 2
DNA thickness (Å)	23.2 ± 0.7	26.4 ± 0.7	27.0 ± 0.5	25.4 ± 0.5
Solvent (%)	90 ± 2	84 ± 2	85 ± 2	85 ± 2

[a] Legends as per Table 2.

Gromelski and Brezesinski who reported a ~18 Å thick DNA layer below DMPE monolayers on a 5 mM $CaCl_2$ sub-phase.[14]

A variety of other models for fitting the reflectivity data were examined – including a model in which ctDNA penetrated the lipid alkyl chain region of the monolayer. It was found that it was only possible to accommodate a very small amount of DNA (max 5% by volume) using physically reasonable constraints (and with fitting performed using the most sensitive contrast). Exactly the same observation was previously noted in modelling of the interaction between DNA and dioctadecyldimethylammonium bromide (DODAB) monolayers.[30] Since the (majority of the) DNA is thus confined at the level of the lipid head groups, we conclude that the DNA molecules are attracted to the air–water interface *via* an electrostatic interaction with the 'pseudo-cationic' lipid head groups, rather than through a hydrophobic driving force. The consistency of the thickness of the DNA layer with varying monolayer surface pressure (12.5–15 Å) is not surprising, given that DNA has been shown to remain in the B-form upon being condensed by DODAB, alone and in combination with both helper lipids.[31]

The DNA content in the ctDNA layer was found to remain relatively constant with a change in surface pressure, and a similar result was previously observed for the interaction between DNA and the monolayers formed from the cationic di-chain lipid, DODAB.[26] The presence of ctDNA, however, has (for reasons that are not entirely clear) a greater effect on the lipid interfacial area at lower surface pressures.

Whereas it is clear that the 4-layer model gives a superior fit to the data by comparison with the 3-layer model, it is important to consider whether this 4-layer model is physically reasonable. In particular, we must ask: is it likely that the DNA in this system would accumulate within a layer some 9 Å away from the lipid head groups? For guidance in this, we may refer to the results obtained in X-ray diffraction and small angle X-ray scattering studies of similar systems. On the basis of their SAXS studies of the calcium-mediated interaction of DNA with multilamellar DPPC vesicles, McManus *et al.*[10] report an interlamellar *d*-spacing of 7.84 nm, with a DPPC bilayer thickness of 4.34 nm, and so determine that the interlamellar water space – wherein the DNA is located – has a thickness of 3.5 nm. Accepting a DNA diameter of ~20 Å, these authors thus calculate that the DNA is separated from the lipid bilayers by a water gap of ~7.5 Å. In the X-ray diffraction and SANS studies reported by Uhríková *et al.*[32] (2012), the DPPC/(20 mM) Ca^{2+}/DNA system is reported to show a *d*-spacing of 8.04 nm, with a bilayer thickness of 5.3 nm. The width of the interlamellar water cushion is thus calculated as 0.74 nm and so – assuming again a DNA diameter of ~20 Å – these authors calculate a DNA-bilayer separation of ~4 Å. Our estimate of a 9 Å gap between the DNA and DSPC layer is perhaps a little high, therefore, but not completely out of line with previous findings. Were we to allow for variation in the interlayer roughnesses in our modelling of the reflectivity data, we might expect that the thickness of the water layer in our 4-layer model might reduce somewhat, at the

Table 6 Structural parameters derived through fitting a four-layer optical matrix model to three contrasts of neutron reflectivity data (d_{70}-DSPC on acmw, d_{83}-DSPC on acmw and d_{70}-DSPC on D_2O) and one contrast of X-ray reflectivity data (h-DSPC on H_2O) for DSPC monolayers spread on a sub-phase containing 20 mM $CaCl_2$ and ctDNA (0.067 mg mL^{-1}) at 295 ± 2 K[a]

Surface pressure (mN m^{-1})	10	20	30	40
Chain thickness (Å)	15.3 ± 0.3	18.9 ± 0.3	20.1 ± 0.3	20.7 ± 0.4
Solvent (%)	0	0	0	0
Head thickness (Å)	10.8 ± 0.5	8.5 ± 0.5	7.9 ± 0.5	7.1 ± 0.6
Solvent (%)	29 ± 4	37 ± 6	23 ± 6	15 ± 8
Water/lipid	5	7	3	2
Thickness of water layer (Å)	9.8 ± 0.8	8.5 ± 0.4	8.4 ± 0.3	9.1 ± 0.4
DNA thickness (Å)	12.5 ± 0.3	14.9 ± 0.7	15.0 ± 0.6	14.1 ± 0.3
Solvent (%)	59 ± 3	67 ± 2	67 ± 2	68 ± 2
Area per DSPC molecule ($Å^2$)	51 ± 2	48 ± 2	47 ± 2	48 ± 2

[a] Legends as per Table 2.

expense of an increase in roughness for one or more of the interfaces. Modelling the reflectivity data with optimisation of the layer thicknesses, their levels of hydration *and* the interfacial roughnesses, however, introduces too many variables to allow determination of an unequivocal solution. We would conclude, therefore, that our 4-layer model is broadly correct, but that our estimate of the DSPC–DNA separation is likely to be a little high.

Conclusions

Co-refinement of the X-ray and neutron reflection data showed that, regardless of the surface pressure of the monolayer, a layer of ctDNA was present below the DSPC lipid head groups and that this ctDNA-containing layer (thickness $\sim$ 12.5–15 Å) was separated from the DSPC head groups by a layer of water of $\sim$9 Å thickness. At all surface pressures the amount of ctDNA present in the layer was in the range 30–40% by volume. No significant re-arrangement of the DSPC film was required to accommodate the presence of the ctDNA, suggesting that the distribution of charges in the lipid film matches well the charge spacing of ctDNA.

Acknowledgements

The authors wish to thank the ESRF (Grenoble, France) and ISIS (Rutherford Appleton Laboratories, Didcot, UK) for granting the necessary beam-time and to the EPSRC and ILL for the award of a studentship to JT. Special thanks goes to the Deuteration and PSCM labs, ILL.

References

1 S. D. Li and L. Huang, *Gene Ther.*, 2006, **13**, 1313–1319.
2 X. Gao, K. S. Kim and D. Liu, *AAPS J.*, 2007, **9**, E92–E104.
3 M. F. Mustapa, S. Grosse, L. Kudsiova, M. Elbs, E.-N. Raiber, J. Wong, A. Brain, H. Armer, A. Warley, M. Keppler, T. Ng, M. J. Lawrence, S. Hart, H. C. Hailes and A. B. Tabor, *Bioconjugate Chem.*, 2009, **20**, 518–532.
4 W. Li and F. C. Szoka Jr, *Pharm. Res.*, 2007, **24**, 438–449.
5 V. G. Budker, Y. A. Kazatchkov and L. P. Naumova, *FEBS Lett.*, 1978, **95**, 143–146.
6 I. Koltover, K. Wagner and C. R. Safinya, *Proc. Natl. Acad. Sci. U. S. A.*, 2000, **97**, 14046–14051.
7 D. P. Kharakoza, R. S. Khusainovaa, A. V. Gorelova and K. A. Dawson, *FEBS Lett.*, 1999, **446**, 27–29.
8 D. E. Leckband, C. A. Helm and J. Israelachvili, *Biochemistry*, 1993, **32**, 1127–1140.
9 X. E. Cai and J. Yang, *Biophys. J.*, 2002, **82**, 357–365.
10 J. J. McManus, J. O. Radler and K. A. Dawson, *Langmuir*, 2003, **19**, 9630–9637.
11 D. Uhríková, A. Lengyel, M. Hanulova, S. S. Funari and P. Balgavy, *Eur. Biophys. J.*, 2007, **36**, 363–375.
12 D. McLoughlin, R. Dias, B. Lindman, M. Cardenas, T. Nylander, K. Dawson, M. Miguel and D. Langevin, *Langmuir*, 2005, **21**, 1900–1907.
13 S. Gromelski and G. Brezesinski, *Phys. Chem. Chem. Phys.*, 2004, **6**, 5551–5556.
14 S. Gromelski and G. Brezesinski, *Langmuir*, 2006, **22**, 6293–6301.
15 L. Cristofolini, T. Berzina, S. Erokhina, O. Konovalov and V. Erokhin, *Biomacromolecules*, 2007, **8**, 2270–2275.
16 S. Kundu, D. Langevin and L. T. Lee, *Langmuir*, 2008, **24**, 12347–12353.
17 C. M. Hollinshead, R. D. Harvey, D. J. Barlow, J. R. P. Webster, A. V. Hughes, A. Weston and M. J. Lawrence, *Langmuir*, 2009, **25**, 4070–4077.
18 A. Nelson, *J. Appl. Crystallogr.*, 2006, **39**, 273–376.
19 R. S. Armen, O. D. Uitt and S. E. Feller, *Biophys. J.*, 1998, **75**, 734–744.
20 H. I. Petrache, S. Feller and J. F. Nagle, *Biophys. J.*, 1997, **72**, 2237–2242.
21 B. Jacrot, *Rep. Prog. Phys.*, 1976, **39**, 911–953.
22 N. O. Petersen, P. A. Kroon, M. Kainoshoa and S. I. Chan, *Chem. Phys. Lipids*, 1975, **14**, 343–349.
23 S. Sunder, D. Cameron, H. H. Mantsch and H. J. Bernstein, *Can. J. Chem.*, 1978, **56**, 2121–2126.
24 C. DeWolf, S. Leporatti and C. Kirsch, *Chem. Phys. Lipids*, 1999, **97**, 129–138.
25 I. Kubo, S. Adachi and H. Maeda, *Thin Solid Films*, 2001, **393**, 80–85.
26 M. Càrdenas, T. Nylander, B. Jonsson and B. Lindman, *J. Colloid Interface Sci.*, 2005, **286**, 166–175.
27 J. Sanchez and A. Badia, *Chem. Phys. Lipids*, 2008, **152**, 24–37.
28 C. Tanford, *The hydrophobic effect and formation of micelles and biological membranes*, Wiley-Interface Science, USA, 2nd edn, 1980.
29 D. M. Small, *J. Lipid Res.*, 1967, **8**, 551–557.
30 A. P. Dabkowska, D. J. Barlow, R. A. Campbell, A. V. Hughes, P. J. Quinn and M. J. Lawrence, *Biomacromolecules*, 2012, **13**, 2391–2401.
31 S. Choosakoonkriang, C. M. Wiethoff, T. J. Anchordoguy, G. S. Koe, J. G. Smith and C. R. Middaugh, *J. Biol. Chem.*, 2001, **276**, 8037–8043.
32 D. Uhríková, N. Kučerka, A. Lengyel, P. Pullmannová, J. Teixeira, T. Murugova, S. S. Funari and P. Balgavý, *J. Phys.*, 2000, **351**, 012011.